AMERICAN SOCIETY FOR MICROBIOLOGY | Applied and Environmental Microbiology®

ENVIRONMENTAL MICROBIOLOGY

# Impact of Seasonal Hypoxia on Activity and Community Structure of Chemolithoautotrophic Bacteria in a Coastal Sediment

**Yvonne A. Lipsewers,[a] Diana Vasquez-Cardenas,[a] Dorina Seitaj,[a] Regina Schauer,[b] Silvia Hidalgo-Martinez,[a] Jaap S. Sinninghe Damsté,[a,c] Filip J. R. Meysman,[a,b,d] Laura Villanueva,[a] Henricus T. S. Boschker[a,b]**

Department of Marine Microbiology and Biogeochemistry and Department of Estuarine and Delta Systems, NIOZ Royal Netherlands Institute for Sea Research, Texel and Yerseke, and Utrecht University, Utrecht, The Netherlands[a]; Section for Microbiology, Department of Bioscience, Aarhus University, Aarhus, Denmark[b]; Faculty of Geosciences, Department of Earth Sciences, Utrecht University, Utrecht, The Netherlands[c]; Department of Environmental, Analytical, and Geo-Chemistry, Vrije Universiteit Brussel (VUB), Brussels, Belgium[d]

**ABSTRACT** Seasonal hypoxia in coastal systems drastically changes the availability of electron acceptors in bottom water, which alters the sedimentary reoxidation of reduced compounds. However, the effect of seasonal hypoxia on the chemolithoautotrophic community that catalyzes these reoxidation reactions is rarely studied. Here, we examine the changes in activity and structure of the sedimentary chemolithoautotrophic bacterial community of a seasonally hypoxic saline basin under oxic (spring) and hypoxic (summer) conditions. Combined 16S rRNA gene amplicon sequencing and analysis of phospholipid-derived fatty acids indicated a major temporal shift in community structure. Aerobic sulfur-oxidizing *Gammaproteobacteria* (*Thiotrichales*) and *Epsilonproteobacteria* (*Campylobacterales*) were prevalent during spring, whereas *Deltaproteobacteria* (*Desulfobacterales*) related to sulfate-reducing bacteria prevailed during summer hypoxia. Chemolithoautotrophy rates in the surface sediment were three times higher in spring than in summer. The depth distribution of chemolithoautotrophy was linked to the distinct sulfur oxidation mechanisms identified through microsensor profiling, i.e., canonical sulfur oxidation, electrogenic sulfur oxidation by cable bacteria, and sulfide oxidation coupled to nitrate reduction by *Beggiatoaceae*. The metabolic diversity of the sulfur-oxidizing bacterial community suggests a complex niche partitioning within the sediment, probably driven by the availability of reduced sulfur compounds ($H_2S$, $S^0$, and $S_2O_3^{2-}$) and electron acceptors ($O_2$ and $NO_3^-$) regulated by seasonal hypoxia.

**IMPORTANCE** Chemolithoautotrophic microbes in the seafloor are dependent on electron acceptors, like oxygen and nitrate, that diffuse from the overlying water. Seasonal hypoxia, however, drastically changes the availability of these electron acceptors in the bottom water; hence, one expects a strong impact of seasonal hypoxia on sedimentary chemolithoautotrophy. A multidisciplinary investigation of the sediments in a seasonally hypoxic coastal basin confirms this hypothesis. Our data show that bacterial community structure and chemolithoautotrophic activity varied with the seasonal depletion of oxygen. Unexpectedly, the dark carbon fixation was also dependent on the dominant microbial pathway of sulfur oxidation occurring in the sediment (i.e., canonical sulfur oxidation, electrogenic sulfur oxidation by cable bacteria, and sulfide oxidation coupled to nitrate reduction by *Beggiatoaceae*). These results suggest that a complex niche partitioning within the sulfur-oxidizing bacterial

**Received** 30 December 2016 **Accepted** 9 March 2017

**Accepted manuscript posted online** 17 March 2017

**Citation** Lipsewers YA, Vasquez-Cardenas D, Seitaj D, Schauer R, Hidalgo-Martinez S, Sinninghe Damsté JS, Meysman FJR, Villanueva L, Boschker HTS. 2017. Impact of seasonal hypoxia on activity and community structure of chemolithoautotrophic bacteria in a coastal sediment. Appl Environ Microbiol 83:e03517-16. https://doi.org/10.1128/AEM.03517-16.

**Editor** Joel E. Kostka, Georgia Institute of Technology

**Copyright** © 2017 American Society for Microbiology. All Rights Reserved.

Address correspondence to Laura Villanueva, laura.villanueva@nioz.nl, or Henricus T. S. Boschker, eric.boschker@nioz.nl.

Y.A.L. and D.V.-C. contributed equally to this article.

Downloaded from http://aem.asm.org/ on July 12, 2018 by Universiteitsbibliotheek Utrecht

community additionally affects the chemolithoautotrophic community of seasonally hypoxic sediments.

**KEYWORDS** *Beggiatoaceae*, CCB cycle, cable bacteria, chemoautotrophy, dark carbon fixation, phospholipid-derived fatty acid (PLFA), rTCA cycle, stable isotope probing (SIP), sulfur oxidation

The reoxidation of reduced intermediates formed during anaerobic mineralization of organic matter is a key process in the biogeochemistry of coastal sediments (1, 2). Many of the microorganisms involved in the reoxidation of reduced compounds are chemolithoautotrophs, which fix inorganic carbon using the chemical energy derived from reoxidation reactions (dark $CO_2$ fixation). In coastal sediments, sulfate reduction forms the main respiration pathway, accounting for 50% to 90% of the organic matter mineralization (1). The reoxidation of the pool of reduced sulfur compounds produced during anaerobic mineralization (dissolved free sulfide, thiosulfate, elemental sulfur, iron monosulfides, and pyrite) hence forms the most important pathway sustaining chemolithoautotrophy in coastal sediments (2, 3).

Various lineages from the *Alphaproteobacteria*, *Gammaproteobacteria*, *Deltaproteobacteria*, and *Epsilonproteobacteria*, including recently identified groups, such as particle-associated *Gammaproteobacteria* and large sulfur bacteria, couple dark $CO_2$ fixation to the oxidation of reduced sulfur compounds in oxygen-deficient marine waters and sediments, in coastal marine sediments, and in lake sediments (4–9). Both chemolithoautotrophic sulfur-oxidizing *Gammaproteobacteria* and sulfur-disproportionating *Deltaproteobacteria* have been identified to play a major role in sulfur and carbon cycling in diverse intertidal sediments (10–12). Hence, chemolithoautotrophic sulfur-oxidizing communities vary between sediment environments, but it is presently not clear as to which environmental factors are actually determining the chemolithoautotrophic community composition at a given site.

Seasonal hypoxia is a natural phenomenon that occurs in coastal areas around the world (13) and provides an opportunity to study the environmental factors controlling sedimentary chemolithoautotrophy. Hypoxia occurs when bottom waters become depleted of oxygen ($<63$ $\mu$mol $O_2 \cdot liter^{-1}$) and has a large impact on the biogeochemical cycling and ecological functioning of the underlying sediments (13). The reduced availability or even absence of suitable soluble electron acceptors ($O_2$ or $NO_3^-$) in the bottom water during part of the year should, in principle, result in a reduction or complete inhibition of sedimentary sulfur reoxidation, and hence, limit chemolithoautotrophy. At present, the prevalence and temporal variations of chemolithoautotrophy have not been investigated in coastal sediments of seasonal hypoxic basins.

Likely, the availability of soluble electron acceptors ($O_2$ and $NO_3^-$) in the bottom water is not the only determining factor of chemolithoautotrophy. A recent study conducted in a seasonally hypoxic saline basin (Lake Grevelingen, The Netherlands) indicated that the intrinsic structure and composition of the sulfur-oxidizing microbial community also determined the biogeochemistry of the sediment (14). In this study, three distinct microbial sulfur oxidation mechanisms were observed throughout a seasonal cycle: (i) electrogenic sulfur oxidation by heterotrophic cable bacteria (*Desulfobulbaceae*), (ii) canonical aerobic oxidation of free sulfide at the oxygen-sulfide interface, and (iii) sulfide oxidation coupled to nitrate reduction by filamentous members of the *Beggiatoaceae* family that store nitrate intracellularly. The consequences of these three mechanisms on the chemolithoautotrophic community have, however, not been studied. The first sulfur-oxidizing mechanism has been shown to affect the chemolithoautotrophic community in sediments only under laboratory conditions (15), while the third mechanisms may directly involve chemolithoautotrophic *Beggiatoaceae*, as some species are known to grow autotrophically (16). Accordingly, we hypothesize that the presence of these sulfur oxidation regimes, as well as the depletion of $O_2$ and $NO_3^-$, will result in a strong seasonality in both the chemolithoautotrophic activity and community structure under natural conditions.

Downloaded from http://aem.asm.org/ on July 12, 2018 by Universiteitsbibliotheek Utrecht

To examine the above-mentioned hypothesis, we conducted a multidisciplinary study with intact sediments of Lake Grevelingen, involving both geochemistry and microbiology. Field sampling was conducted during spring (oxygenated bottom waters) and summer (oxygen-depleted bottom waters). The dominant sulfur oxidation mechanism was geochemically characterized by sediment microsensor profiling ($O_2$, $H_2S$, and pH), whereas the abundance of cable bacteria and *Beggiatoaceae* was determined with fluorescence *in situ* hybridization (FISH). General bacterial diversity was assessed by 16S rRNA gene amplicon sequencing and the analysis of phospholipid-derived fatty acids (PLFA). PLFA analysis combined with $^{13}C$-stable isotope probing (PLFA-SIP) provided the activity and community composition of chemolithoautotrophs in the sediment. This approach was complemented by the analysis of genes involved in dark $CO_2$ fixation, i.e., characterizing the diversity and abundance of the genes *cbbL* and *aclB* that code for key enzymes in Calvin-Benson-Bassham (CBB) and reductive tricarboxylic acid (rTCA) carbon fixation pathways. This multidisciplinary research showed strong temporal and spatial shifts of the chemolithoautotrophic composition and activity in relation to the seasonal hypoxia and the main sulfur oxidation mechanisms present in the sediments of the marine Lake Grevelingen.

## RESULTS

**Geochemical characterization.** The seasonal variation of the bottom-water oxygen concentration in Lake Grevelingen strongly influenced the pore water concentrations of $O_2$ and $H_2S$. In March, bottom waters were fully oxygenated at all stations (299 to 307 $\mu$mol · liter$^{-1}$), oxygen penetrated 1.8 to 2.6 mm deep in the sediment, and no free sulfide was recorded in the first few centimeters (Table 1). The width of the suboxic zone, operationally defined as the sediment layer located between the oxygen penetration depth (OPD) and the sulfide appearance depth (SAD), varied between 16 and 39 mm across the three stations in March 2012. In contrast, in August, oxygen was strongly depleted in the bottom waters at station S1 ($<$0.1 $\mu$mol · liter$^{-1}$) and station S2 (11 $\mu$mol · liter$^{-1}$), and no $O_2$ could confidently be detected by microsensor profiling in the surface sediment at these two stations. At station S3, the bottom-water $O_2$ level remained higher (88 $\mu$mol · liter$^{-1}$), and oxygen penetrated down to 1.1 mm. In August, free sulfide was present near the sediment-water interface at all three stations, and the accumulation of sulfide in the pore water increased with water depth (Fig. 1a). Depth pH profiles showed much larger variation between stations in March than those in August (Fig. 1a). The pH profiles at S1 and S3 in March were similarly characterized by the highest values in the oxic zone and low pH values (pH $<$ 6.5) in the suboxic zone. The pH depth profile at S2 showed an inverse pH profile, with a pH minimum in the oxic layer and a subsurface maximum below. The pH profiles at S1 and S3 in August 2012 showed a gradual decline in pH with depth, while the pH profile at S2 in August was more or less constant with depth.

**Bacterial diversity by 16S rRNA gene amplicon sequencing.** The general diversity of bacteria was assessed by 16S rRNA gene amplicon sequencing analysis, which was applied to the surface sediments (0 to 1 cm) of all stations in both March and August. Approximately 50% of the reads were assigned to three main clades: *Gammaproteobacteria*, *Deltaproteobacteria*, and *Epsilonproteobacteria* (Fig. 2). The remaining reads were distributed among the orders *Bacteroidetes* (14%), *Planctomycetes* (6%), *Alphaproteobacteria* (3%), other orders (20%), the candidate phylum WS3 (2%), and unassigned (5%) (given as the average of the three stations and both seasons).

Reads classified within the *Gammaproteobacteria* were more abundant in March under oxygenated bottom-water conditions than in August (Fig. 2). The majority of these reads were assigned to the orders *Alteromonadales*, *Chromatiales*, and *Thiotrichales*. *Alteromonadales* includes chemoheterotrophic bacteria that are either strict aerobes or facultative anaerobes (17). Phylogenetic comparison revealed that the reads assigned to the *Chromatiales* group were closely related to the *Granulosicoccaceae*, *Ectothiorhodospiraceae*, and *Chromatiaceae* families (see Fig. S1 in the supplemental material). Reads falling in the *Thiotrichales* group were closely related to sulfur-oxidizing

Downloaded from http://aem.asm.org/ on July 12, 2018 by Universiteitsbibliotheek Utrecht

**TABLE 1** Geochemical characterization, chemoautotrophy rates, and quantification of cable bacteria and *Beggiatoaceae* in the three stations in Lake Grevelingen for spring (March) and summer (August)

| Station by mo | Temp (°C) | Bottom-water concn ($\mu$M) of[a]: $O_2$ | Bottom-water concn ($\mu$M) of[a]: $NO_3^-$ | DOU (mmol $O_2 \cdot m^{-2} \cdot day^{-1}$)[b] | Depth (mm)[c]: OPD (mean ± SD) | Depth (mm)[c]: SAD (mean ± SD) | Depth (mm)[c]: Suboxic zone** | pH signature[d] | Chemolithoautotrophy rate (mmol $C \cdot m^{-2} \cdot day^{-1}$) | Cable bacteria biovolume ($mm^3 \cdot cm^{-2}$)[e] | *Beggiatoaceae* biovolume ($mm^3 \cdot cm^{-2}$) |
|---|---|---|---|---|---|---|---|---|---|---|---|
| March | | | | | | | | | | | |
| 1 | 5 | 299 (oxic) | 28.2 | 18.2 ± 1.7 | 1.8 ± 0.04 | 17.5 ± 0.7 | 16 | e-SOx | 3.1 ± 0.5 | 2.55 | 0.02 |
| 2 | 5 | 301 (oxic) | 27.9 | 15.8 ± 3.1 | 2.6 ± 0.65 | 21.3 ± 2.5 | 19 | Nitrate-storing *Beggiatoaceae* | 1.9 ± 0.1 | ND | 0.11 |
| 3 | 5 | 307 (oxic) | 27.7 | 17.1 ± 5.7 | 2.4 ± 0.4 | 41.8 ± 8.6 | 39 | e-SOx | 1.4 ± 0.3 | 2.08 | 0.05 |
| August | | | | | | | | | | | |
| 1 | 17 | 0 (anoxic) | 1.7 | 0 | 0 | 0.9 ± 1.1 | 0.9 | Sulfate reduction/canonical sulfur oxidation | 0.2 ± 0.1 | 0.11 | 0.001 |
| 2 | 17 | 12 (hypoxic) | 11.6 | 0 | 0 | 0.6 ± 0 | 0.6 | | 0.8 ± 0.3 | ND | 3.24 |
| 3 | 19 | 88 (hypoxic) | 10.6 | 13.9 ± 2.1 | 1.1 ± 0.1 | 4.2 ± 2.7 | 3 | | 1.1 ± 0.5 | 0.003 | 0.004 |

[a]Bottom water is classified as anoxic with $O_2$ concentration below 1 $\mu$M and hypoxic below 63 $\mu$M.
[b]DOU, dissolved $O_2$ uptake.
[c]OPD, $O_2$ penetration depth; SAD, $\Sigma H_2S$ appearance depth. The thickness of the suboxic zone is defined as the average SAD minus the average OPD.
[d]pH signature serves to indicate the sulfur-oxidizing mechanism that dominates the pore water chemistry, as described by Seitaj et al. (14). e-SOx, electrogenic sulfur oxidation.
[e]ND, not determined.





Downloaded from http://aem.asm.org/ on July 12, 2018 by Universiteitsbibliotheek Utrecht

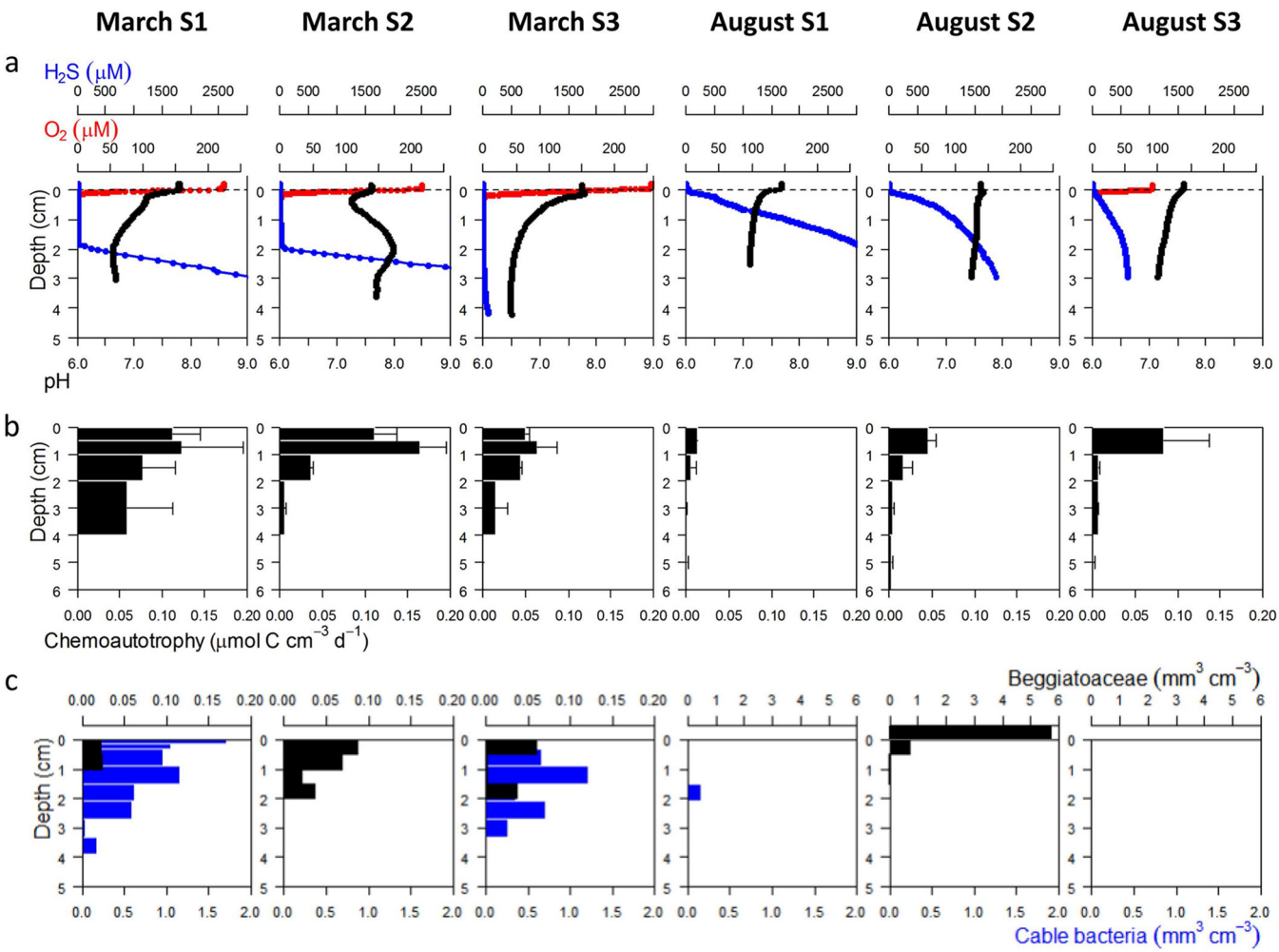


**FIG 1** Geochemical fingerprint, shown by pH, $H_2S$, and $O_2$ profiles (a), chemoautotrophy depth profiles (b), and biovolumes of filamentous *Beggiatoaceae* (black) and cable bacteria (blue) (c) in sediment of Lake Grevelingen for March and August in all three stations (note change in scale for *Beggiatoaceae* between March and August). S1, station 1 (34 m); S2, station 2 (23 m); S3, station 3 (17 m).

bacteria from the *Thiotrichaceae* family, with 30% of the sequences related to the genera "*Candidatus* Isobeggiatoa," "*Candidatus* Parabeggiatoa," and *Thiomargarita* (see Fig. S2 in the supplemental material). It has been recently proposed that the genera *Beggiatoa*, *Thiomargarita*, and *Thioploca* should be reclassified into the originally published monophyletic family *Beggiatoaceae* (18, 19); here, therefore, these genera are referred to as *Beggiatoaceae*. Most of the reads assigned to the *Beggiatoaceae* came from station S2 in spring, whereas the percentage of reads assigned to sulfur oxidizers from the order *Thiotrichales* decreased in August when oxygen concentrations in the bottom water were low.

Within the *Deltaproteobacteria*, reads were assigned to the orders *Desulfarculales* and *Desulfobacterales* (see Fig. S3 in the supplemental material). Reads within the order *Desulfobacterales* were mainly assigned to the families *Desulfobacteraceae* (between 10 and 20%) and *Desulfobulbaceae* (~5%) (Fig. 2). Additional phylogenetic comparison revealed that within the *Desulfobulbaceae*, 60% of reads, obtained from the three stations in both seasons, clustered within the genus *Desulfobulbus*, of which 30% were related to the electrogenic sulfur-oxidizing cable bacteria (see Fig. S4 in the supplemental material). Overall, the relative abundance of reads assigned to the *Desulfobulbaceae* family was similar between the two seasons at S2 and S3, whereas at S1, the percentage of reads was approximately 4.5-fold higher in March than in August (Fig. 2). In contrast, the relative abundance of reads assigned to the *Desulfarculales* and

Downloaded from http://aem.asm.org/ on July 12, 2018 by Universiteitsbibliotheek Utrecht

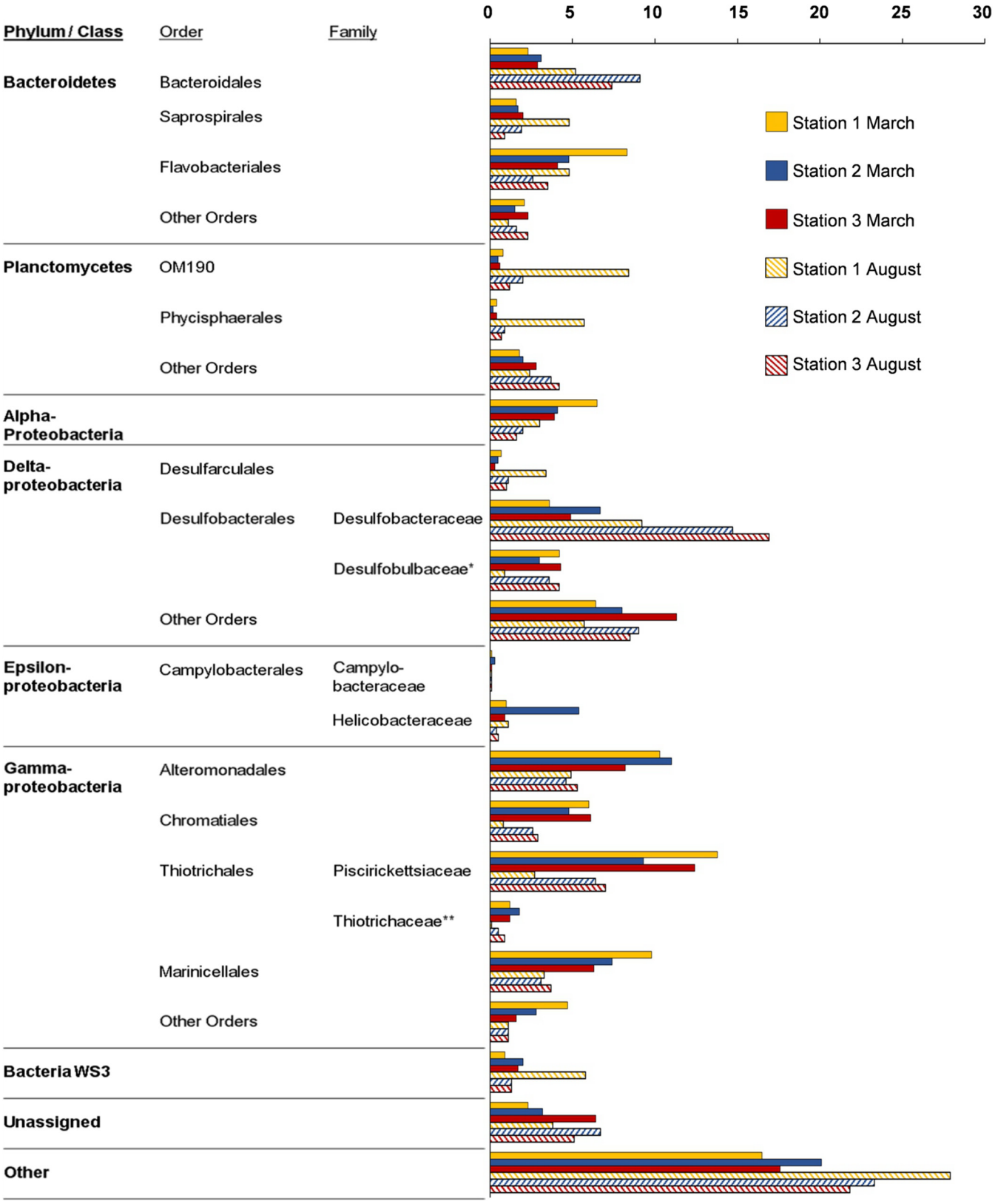


**FIG 2** Percentages of total bacterial 16S rRNA gene reads at stations S1 (yellow), S2 (blue), and S3 (red) in March (filled) and August (hatched). Classified bacterial phyla, classes, and orders >3% of the total bacteria reads (in March or August) are reported (exception: family *Thiotrichaceae*, <3%). *, including cable bacteria; **, including *Beggiatoaceae*.

Downloaded from http://aem.asm.org/ on July 12, 2018 by Universiteitsbibliotheek Utrecht

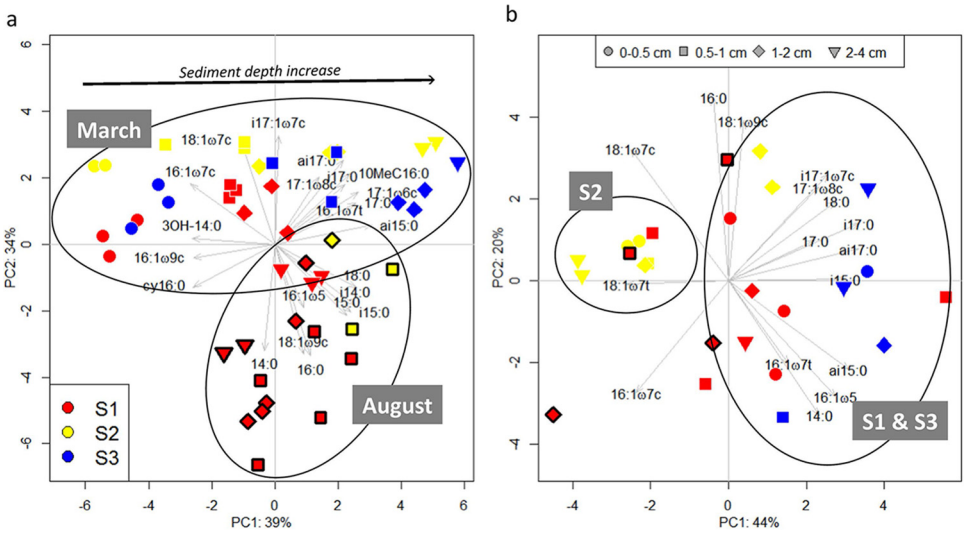


**FIG 3** Principal-component analysis (PCA) of relative PLFA concentrations (a) and of $^{13}C$ incorporation into PLFA (b) in sediments from the three stations in March (no border) and August (black border). The percentage of variability explained by the first two principal components (PC) is indicated on each axis. Red, station S1; yellow, station S2; blue, station S3. Symbols indicate sediment depth, as seen in plot.

*Desulfobacteraceae* increased in August during hypoxia (Fig. 2), and a phylogenetic comparison revealed typical sulfate-reducing genera *Desulfococcus*, *Desulfosarcina*, and *Desulfobacterium*, indicative of anaerobic metabolism (Fig. S5a to c).

All *Epsilonproteobacteria* reads, such as the *Campylobacteraceae* and *Helicobacteraceae* families, were assigned to the order *Campylobacterales*. Phylogenetic comparison showed that the reads were closely related to the genera *Sulfurovum*, *Sulfurimonas*, *Sulfurospirillum*, and *Arcobacter* (see Fig. S6a to d in the supplemental material), all capable of sulfur oxidation with oxygen or nitrate (20). The percentage of reads assigned to the *Epsilonproteobacteria* in August was lower than that in March, with the highest numbers present at S2 in March (~6%) (Fig. 2).

**Bacterial community structure by PLFA.** The relative concentrations of phospholipid-derived fatty acids (PLFAs) were determined to a depth of 6 cm and were analyzed by principal-component analysis (PCA) to determine differences in bacterial community structure (Fig. 3). A total of 22 individual PLFAs, each contributing more than 0.1% to the total PLFA biomass, were included in this analysis. Samples with low total PLFA biomass (less than one standard deviation below the mean of all samples) were excluded. The PCA indicated that 73% of the variation within the data set was explained by the first two principal components (PCs). While PC1 correlated with sediment depth (particularly for the March samples), PC2 clearly exposed differences in the bacterial community structure between seasons (Fig. 3a). Surface sediments (0 to 1 cm) were characterized by high relative concentrations of $C_{16}$ and $C_{18}$ monounsaturated PLFAs. In contrast, ai15:0, i17:1$\omega$7c, and 10Me16:0 were more abundant in deeper sediments (see Fig. S7a in the supplemental material). The surface sediment showed an increased contribution of iso, anteiso, and branched PLFAs in August relative to March, and this was more similar to the deeper sediments from March (Fig. 3a). Nonetheless, August sediments also showed higher abundances of 16:0, 14:0, and 18:1$\omega$9c than in the deeper sediment layers in March (Fig. S7a).

**Chemolithoautotrophic activity and community by [$^{13}C$]phospholipid fatty acid analysis.** Incorporation of $^{13}C$-labeled dissolved inorganic carbon was found in bacterial PLFAs after 24 to 40 h of incubation (Fig. S7b). Depth-integrated dark $CO_2$ fixation rates based on $^{13}C$ incorporation (Table 1) showed a significant difference between seasons and stations ($P = 0.0005$). In March, chemolithoautotrophy increased with water depth, while in August, the opposite trend was observed. The dark $CO_2$ fixation rate in March for S1 was the highest across all seasons and stations but

Downloaded from http://aem.asm.org/ on July 12, 2018 by Universiteitsbibliotheek Utrecht

dropped by one order of magnitude in August. In contrast, at the intermediate station (S2), the dark $CO_2$ fixation rate was only two times higher in March than in August, while at the shallowest station (S3), the depth-integrated rates were not significantly different between seasons ($P = 0.56$).

The depth distribution of the chemolithoautotrophic activity also differed between seasons ($P = 0.02$; Fig. 1b). In August, the chemolithoautotrophic activity was restricted to the upper centimeter of the sediment at all stations, while in March, chemolithoautotrophic activity was measured deep into the sediment (up to 4 cm). At stations S1 and S3 during March, the activity depth profile showed high activities down to 4 cm, whereas at S2, chemolithoautotrophy only extended down to 2 cm, with the highest activity in the top 1 cm. This distinction between the depth distributions of chemolithoautotrophy at S2 versus S1/S3 in March correlated with the distinct pH profiles observed for S2 versus S1/S3 (Fig. 1c).

The PLFA $^{13}$C-labeled fingerprints were analyzed by PCA to identify differences in the chemolithoautotrophic community. Only PLFAs that contributed more than 0.1% to the total $^{13}$C incorporation and sediment layers that showed chemolithoautotrophy rates higher than 0.01 $\mu$mol C $\cdot$ cm$^{-3}$ $\cdot$ day$^{-1}$ were taken into account in this analysis. Because chemolithoautotrophy rates were low in August, the PCA mainly analyzed the chemolithoautotrophic communities in March (Fig. 3b). Within the data set, 64% of the variation was explained by two principal components. PC1 revealed a clear differentiation between station S2 and stations S1 and S3 (Fig. 3b), in agreement with the distinct pH profiles described for March (Fig. 1a). S2 sediment horizons showed a higher contribution of monounsaturated $C_{16}$ and $C_{18}$ fatty acids, whereas sediments from S1 and S3 revealed an increased $^{13}$C incorporation into fatty acids with iso and anteiso $C_{15}$ and saturated $C_{14}$ PLFAs (Fig. S7c); together, these results indicate distinct chemolithoautotrophic microbial assemblages between S2 and S1/S3. On the contrary, the three sediment samples from August (which had sufficient $^{13}$C incorporation for the analysis) did not cluster in the PCA and exhibited divergent PLFA profiles; thus, the chemolithoautotrophic bacterial community for August could not be characterized further based on PLFA analysis.

**Chemolithoautotrophic carbon fixation pathways.** Various $CO_2$ fixation pathways are used by autotrophic bacteria (for detailed reviews, see references 23 and 27). The CBB pathway is utilized by cyanobacteria and many aerobic or facultative aerobic proteobacteria of the alpha, beta, and gamma subgroups, whereas the rTCA pathway operates in anaerobic or microaerobic members of phyla, such as *Chlorobi*, *Aquificae*, *Proteobacteria* of the delta and epsilon subgroups, and *Nitrospirae* (23). The spatial and temporal distribution of bacteria possessing these two autotrophic carbon fixation pathways was studied by quantifying the abundance of the *cbbL* gene (CBB pathway) (24) and *aclB* gene (rTCA pathway) (based on reference 20 but modified in this study) by quantitative PCR down to 5 cm sediment depth (Fig. 4).The diversity of *cbbL* and *aclB* gene sequences obtained from the surface sediments (0 to 1 cm) was analyzed (Fig. 5).

Significant differences were found in the abundances of *cbbL* and *aclB* genes ($P = 5.7 \times 10^{-7}$) and between season ($P = 0.002$) but not between stations (Fig. 4). The amount of the *cbbL* gene copies was at least 2-fold higher than that of the *aclB* gene in March and August in all stations ($P = 5 \times 10^{-5}$). In March, the depth profiles of the *cbbL* gene showed a similar trend at stations S1 and S3, with a decreasing gene abundance from the surface toward deeper layers, but depth-integrated abundance of the *cbbL* gene was more than 2-fold higher at S1 than at S3 (Fig. 4a). The depth distribution of the *cbbL* gene at the deepest station (S1) differed between seasons ($P = 0.004$), with lower gene copy numbers in the top 4 cm in August (Fig. 4a). In contrast, at the shallow station (S3), which experiences fewer seasonal fluctuations in bottom-water $O_2$, the *cbbL* gene copy number did not differ significantly between seasons ($P = 0.4$), except for a sharp decrease in the top centimeter of the sediment. At station S2, the abundance and depth distribution of *cbbL* gene copies were similar between the two seasons ($P = 0.3$). All detected *cbbL* gene sequences clustered with uncultured

Downloaded from http://aem.asm.org/ on July 12, 2018 by Universiteitsbibliotheek Utrecht

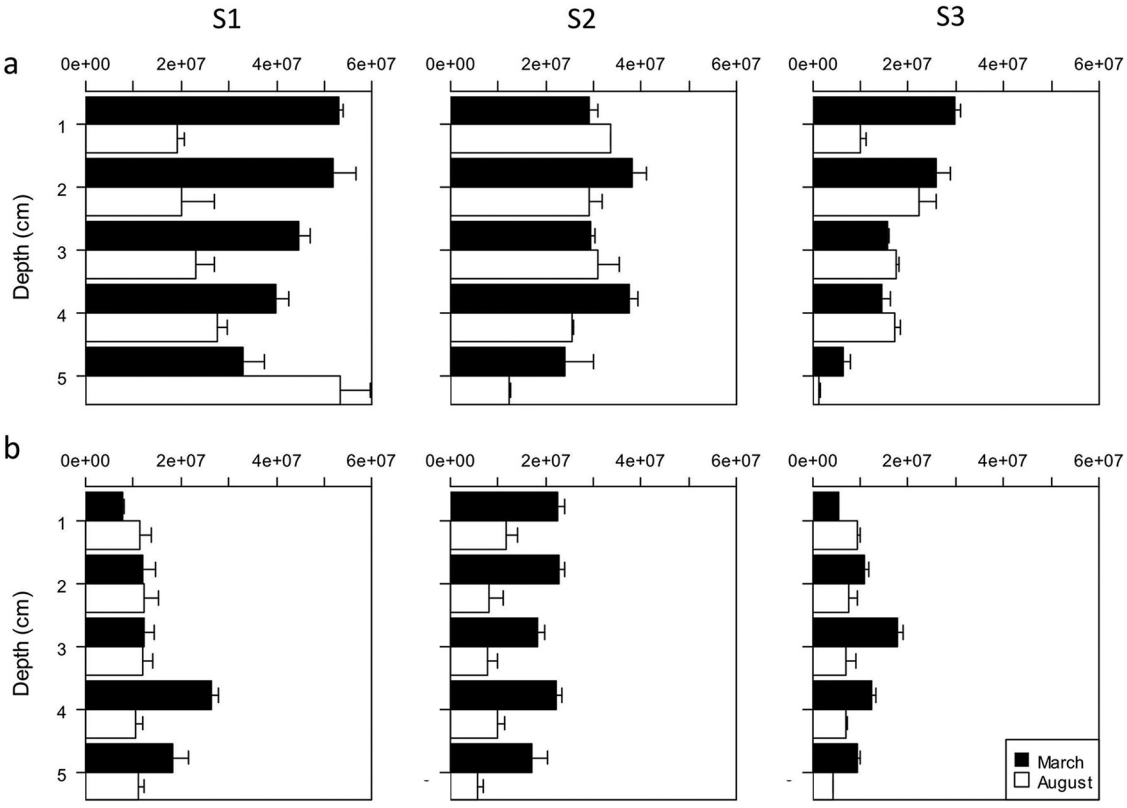


**FIG 4** Abundance (in copies per gram) of two carbon fixation pathway genes with sediment depth (in centimeters) for S1 (left), S2 (middle), and S3 (right) with the RuBisCO *cbbL* gene (a) and ATP citrate lyase *aclB* gene (b) (black, March; white, August). The error bars represent the standard deviations of qPCR triplicates.

gammaproteobacterial clones, assigned to the orders *Chromatiales* and *Thiotrichales* (both *cbbL1* and *cbbL2* clusters) reported in intertidal sediment from Lowes Cove, ME (24).

The abundance of the *aclB* gene significantly differed between months ($P = 0.0004$) and stations ($P = 0.04$). Similar depth profiles of the *aclB* gene were detected at stations S1 and S3, with subsurface maxima in deeper sediments (at 3 to 4 cm and 2 to 3 cm deep for S1 and S3, respectively, Fig. 4b). Station S2 showed the highest *aclB* gene abundance in March, which remained constant with sediment depth ($P = 0.86$). In August, *aclB* gene abundance decreased substantially at S2 ($P < 0.001$). All stations showed a uniform distribution of the *aclB* gene abundance with depth in August. Bacterial *aclB* gene sequences in surface sediments (0 to 1 cm) of all stations were predominantly related to *aclB* sequences of *Epsilonproteobacteria* (Fig. 5b). Within the *Epsilonproteobacteria*, sequences clustered in six different subclusters and were mainly affiliated with bacteria in the order *Campylobacterales*, i.e., to the genera *Sulfuricurvum*, *Sulfurimonas*, *Thiovulum*, and *Arcobacter*, and macrofaunal endosymbionts. As observed for the *cbbL* gene, no clustering of sequences was observed according to station or season (Fig. 5b).

**Quantification of cable bacteria and filamentous *Beggiatoaceae*.** We performed a detailed microscopy-based quantification of the biovolume of sulfur-oxidizing cable bacteria and filamentous *Beggiatoaceae*, because both groups have been reported to govern the sediment geochemistry and sulfur cycling in sediments of Lake Grevelingen (14) and thus are likely to influence the chemolithoautotrophic community. Biovolume data of both filamentous bacteria for S1 have been reported before (14), whereas data for S2 and S3 are novel results from the 2012 campaign. In March, high biovolumes of cable bacteria were detected at S1 and S3 (Table 1), with filaments present throughout the suboxic zone to a maximum depth of 4 cm (Fig. 1c). At the same time, cable

Downloaded from http://aem.asm.org/ on July 12, 2018 by Universiteitsbibliotheek Utrecht

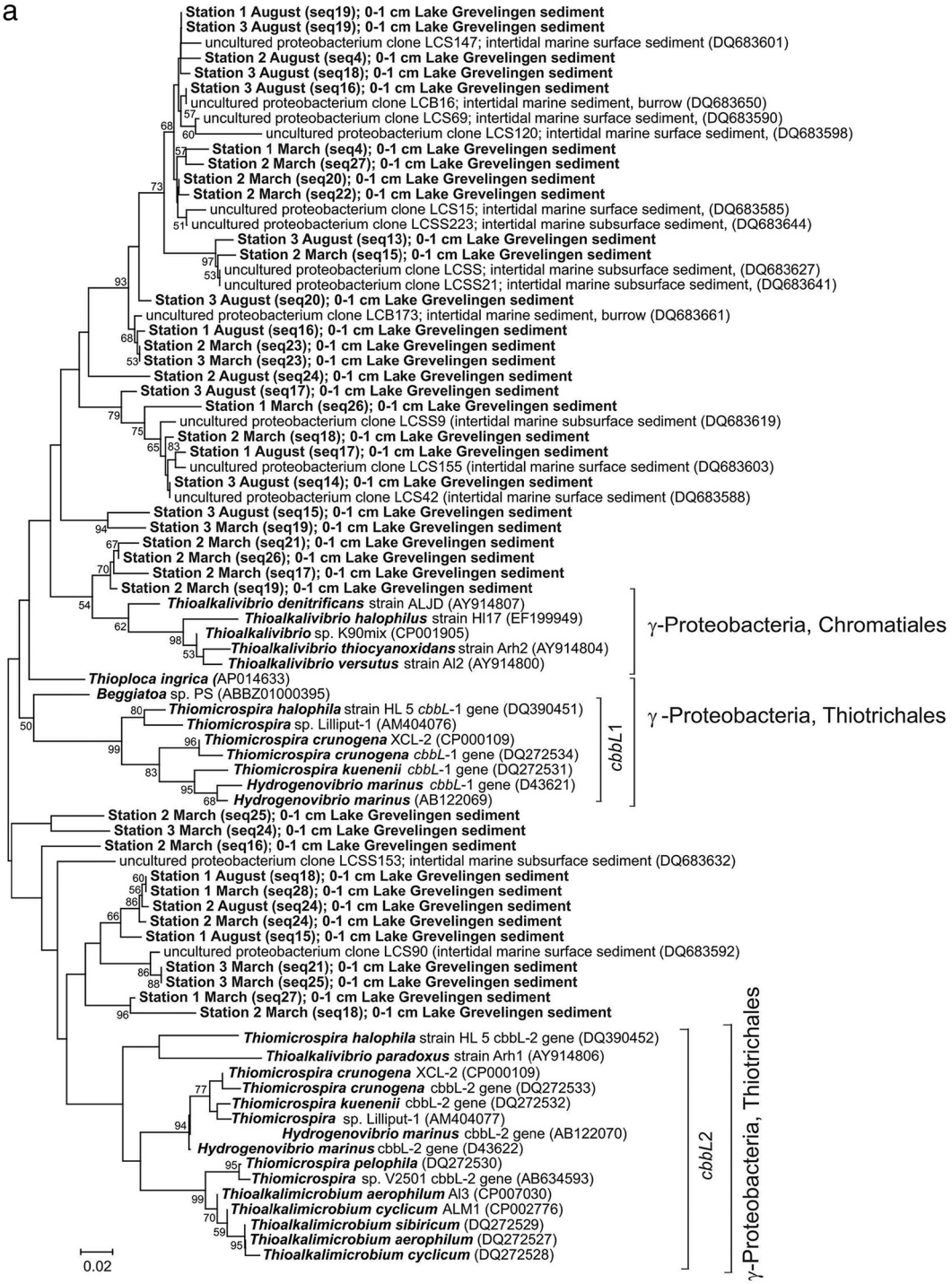


**FIG 5** Phylogenetic tree (amino acid-based) of *cbbL* gene (a) and *aclB* gene (b) sequences retrieved in this study and closest relatives. Bold, sequences of stations S1, S2, and S3 in March and August and closest known relatives. The scale bar indicates 2% (a) and 5% (b) sequence divergence. Accession numbers are shown in parentheses to the right of organism names.

bacteria were absent at S2 (Fig. 1c). In August, cable bacteria were detected only between 1 and 2 cm deep at the deepest station (S1), albeit at abundances that were close to the detection limit of the technique. *Beggiatoaceae* were found at all three stations in March, although the biovolume at S2 was one order of magnitude higher than at the other two stations (Table 1). At station S2, *Beggiatoaceae* were uniformly distributed up to the sulfide appearance depth (Fig. 1c). In August, *Beggiatoaceae* were

Downloaded from http://aem.asm.org/ on July 12, 2018 by Universiteitsbibliotheek Utrecht


**FIG 5** (Continued)

Downloaded from http://aem.asm.org/ on July 12, 2018 by Universiteitsbibliotheek Utrecht

no longer detectable at stations S1 and S3 (Table 1), while at S2, filaments were no longer found in deeper sediment but formed a thick mat at the sediment-water interface (Fig. 1c).

## DISCUSSION

**Temporal shifts of chemolithoautotrophy and the associated bacterial assemblages.** Together, our geochemical and microbiological characterization of the sediments of Lake Grevelingen indicates that the availability of electron acceptors ($O_2$ and $NO_3^-$) constitutes the main environmental factor controlling the activity of the chemolithoautotrophic bacterial community. In the deeper basins of Lake Grevelingen (below water depth of 15 m), the electron acceptor availability changes on a seasonal basis due to the establishment of summer hypoxia (14, 26). In March, when high oxygen levels are found in the bottom waters, the chemolithoautotrophy rates were substantially higher than those in August, when oxygen in the bottom water was depleted to low levels (Fig. 1b and Table 1). Moreover, in August, the chemolithoautotrophy rates showed a clear decrease with water depth (from S3 to S1) in line with the decrease in the bottom-water oxygen concentration over depth.

The 16S rRNA gene amplicon sequencing analysis in our study reveals that the response of the chemolithoautotrophic bacterial community in the surface sediments of Lake Grevelingen is associated with the seasonal changes in bottom-water oxygen (Fig. 2). In general, Lake Grevelingen surface sediments harbor a distinct microbial community comparable to other surface sediments, such as coastal marine (North Sea), estuarine, and Black Sea sediments (8, 9, 12), studied by 16S rRNA gene amplicon sequencing analysis.

In March, with oxic bottom waters, the microbial community in the top centimeter of the sediment at all three stations was characterized by high abundances of *Epsilonproteobacteria* and *Gammaproteobacteria*, which are known chemolithoautotrophic sulfur oxidizers (e.g., capable of oxidizing sulfide, thiosulfate, elemental sulfur, and polythionates) using oxygen or nitrate as an electron acceptor (20, 28–30). In August, the lack of electron acceptors ($O_2$ and $NO_3^-$) in the bottom water was accompanied by a decrease in the relative abundances of these *Gammaproteobacteria* and *Epsilonproteobacteria*. At the same time, the numbers of reads related to the *Desulfobacteraceae* family increased in the top centimeter of the sediment, and a shift in the microbial community structure toward sulfate-reducing bacteria related to the genera *Desulfococcus* and *Desulfosarcina* was evident. In coastal sediments, these genera are characteristic in deeper sediment layers experiencing anaerobic mineralization (31–33), and thus, they are not unexpected in surface sediments under strongly hypoxic (S2) and anoxic (S1) conditions encountered in August. Shifts in PLFA patterns are in agreement with the temporal difference in the bacterial community (Fig. 3a), with more PLFAs found in *Gammaproteobacteria* and *Epsilonproteobacteria* in March (i.e., 16:1$\omega$7c and 18:1 $\omega$7c [34]), as opposed to more PLFAs found in sulfate-reducing bacteria in the *Deltaproteobacteria* in August (i.e., ai15:0, i17:1$\omega$7c, 10Me16:0 [35–37]). However, sediments below the OPD in March have PLFA patterns that are more similar to those of surface sediments in August, in agreement with the observation that anaerobic metabolism, such as sulfate reduction, prevails in deeper anoxic sediments also in March.

**Spring activity and diversity of chemolithoautotrophic bacteria.** Although the availability of soluble electron acceptors ($O_2$ and $NO_3^-$) in the bottom water is important, our data show that it cannot be the only structuring factor of the chemolithoautotrophic communities. In March 2012, all three stations examined experienced similar bottom-water $O_2$ and $NO_3^-$ concentrations (Table 1), but still, substantial differences were observed in the compositions of the chemolithoautotrophic communities, as determined by PLFA-SIP (Fig. 3b), as well as in the depth distribution of the chemolithoautotrophy rates in the sediment (Fig. 1b). We attribute these differences to the presence of specific sulfur oxidation mechanisms that are active in the sediments of Lake Grevelingen (14). In March 2012, based on FISH counts and microsensor profiles, two separate sulfur oxidation regimes were active at the sites investigated: sites S1 and

Downloaded from http://aem.asm.org/ on July 12, 2018 by Universiteitsbibliotheek Utrecht

S3 were impacted by electrogenic sulfur oxidation by cable bacteria, while site S2 was dominated by sulfur oxidation via nitrate-storing filamentous *Beggiatoaceae*. Each of these two regimes is characterized by a specific sulfur-oxidizing microbial community and a particular depth distribution of the chemolithoautotrophy. We now discuss these two regimes separately in more detail.

**Electrogenic sulfur oxidation.** In March, stations S1 and S3 (Fig. 1a) showed the geochemical fingerprint of electrogenic sulfur oxidation (e-SOx), consisting of a centimeter-wide suboxic zone that is characterized by acidic pore waters (pH $<$ 7) (38, 39). Electrogenic sulfur oxidation is attributed to the metabolic activity of cable bacteria (40), which are long filamentous bacteria related to the sulfate-reducing genus *Desulfobulbus* that extend centimeters deep into the sediment (25). The observed depth distribution of cable bacteria at S1 and S3 (Fig. 1c) was congruent with the geochemical fingerprint of e-SOx. Cable bacteria couple the oxidation of sulfide in deeper layers to the reduction of oxygen near the sediment-water interface by channeling electrons along their longitudinal axis (long-distance electron transport). Note that stations S1 and S3 also contained some *Beggiatoaceae*. However, they attained low biovolumes and were only found at certain depths, suggesting that they did not play a significant role in sulfur oxidation.

When e-SOx was present in the sediment (sites S1 and S3 in March), the chemolithoautotrophic activity penetrated deeply into the sediment and was evenly distributed throughout the suboxic zone (Fig. 1b). These field observations confirm previous laboratory incubations in which cable bacteria were induced under oxic conditions in homogenized sediments, and a highly similar depth pattern of deep chemolithoautotrophy was noted (15). This deep dark $CO_2$ fixation is unexpected in two ways. First, cable bacteria are likely not responsible for the deep $CO_2$ fixation, although they do perform sulfur oxidation, as cable bacteria from Lake Grevelingen have been shown to incorporate organic carbon rather than inorganic carbon (15). Second, chemolithoautotrophy is generally dependent on reoxidation reactions, but there is no transport of oxygen or nitrate to centimeters of depth in these cohesive sediments, and so the question is: how can chemolithoautotrophic reoxidation occur in the absence of suitable electron acceptors?

To reconcile these observations, it was proposed that in incubated electroactive sediments from Lake Grevelingen, heterotrophic cable bacteria can form a sulfur-oxidizing consortium with chemolithoautotrophic *Gammaproteobacteria* and *Epsilonproteobacteria* throughout the suboxic zone (15). The results obtained in our study provide various lines of evidence that support the existence of such a consortium in intact sediment cores. The PLFA-SIP patterns at S1 and S3 (Fig. 3b) showed major $^{13}C$ incorporation in PLFAs which are present in sulfur-oxidizing *Gammaproteobacteria* and *Epsilonproteobacteria* (21, 22, 29, 41), and this occurred throughout the top 5 cm of the sediment, corresponding to the zone of e-SOx activity. In addition, the depth profiles of genes involved in dark $CO_2$ fixation (Fig. 4) revealed chemolithoautotrophic *Gammaproteobacteria* using the CBB cycle as well as *Epsilonproteobacteria* using the rTCA cycle, which confirms the potential dark $CO_2$ fixation by both bacterial groups deep in the sediment. The higher abundance of *cbbL* genes at S1 than at S3 indicates a greater chemolithoautotrophic potential of *Gammaproteobacteria*, which may explain the 2-fold-higher total chemolithoautotrophy rate encountered at S1. Moreover, the peak in *aclB* gene abundance found in deeper sediment suggests that *Epsilonproteobacteria* could play an important role in sulfur oxidation in the deeper suboxic zone in both stations. Clearly, a consortium could sustain the high rates of chemolithoautotrophy throughout the suboxic zone. It has been speculated that chemolithoautotrophs use the cable bacteria as an electron sink in the absence of an electron acceptor, like $O_2$ or $NO_3^-$, in centimeter-deep sediments (15). However, the question still remains as to how *Gammaproteobacteria* and *Epsilonproteobacteria* are metabolically linked to the cable bacteria (Fig. 6).

Downloaded from http://aem.asm.org/ on July 12, 2018 by Universiteitsbibliotheek Utrecht

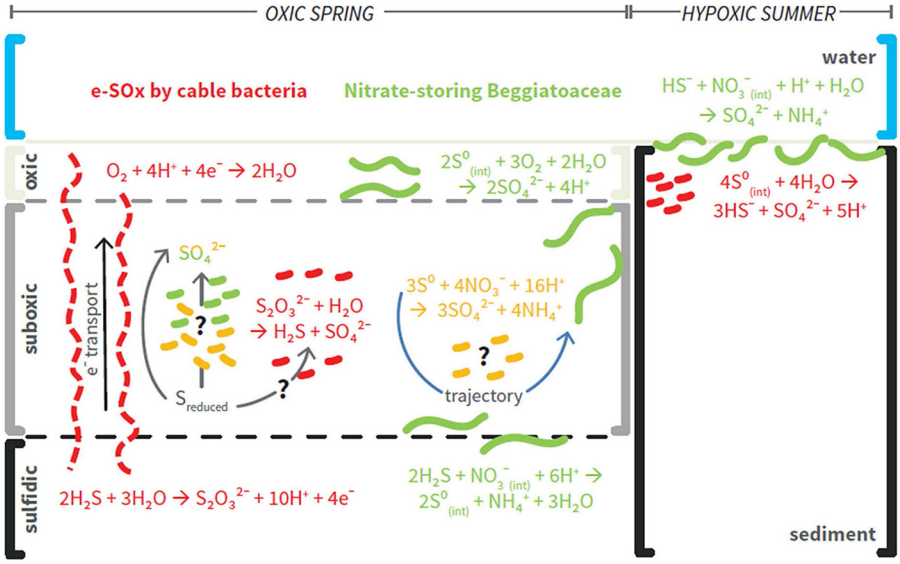


**FIG 6** Schematic representation of the main sulfur oxidation mechanisms by chemoautotrophic bacteria under oxic conditions in spring (left) and under hypoxic conditions in summer (right) in marine Lake Grevelingen single-celled and filamentous sulfur-oxidizing bacteria. Yellow, *Epsilonproteobacteria*; green, *Gammaproteobacteria*; red, *Deltaproteobacteria*. Gray arrows represent possible reoxidation processes by chemoautotrophic bacteria, and the color of the reaction indicates the bacterial group involved; blue arrow, trajectory of filamentous *Beggiatoaceae* (thick green lines) from the surface to the sulfide horizon and back up to the surface; black arrow, long-distance electron transport by cable bacteria (red dashed lines).

In March, stations S1 and S3 also showed a higher contribution of fatty acids occurring in the sulfate-reducing *Deltaproteobacteria* (11, 36, 42) than the PLFA-SIP profiles at station S2 (Fig. 3b). *Deltaproteobacteria*, such as *Desulfobacterium autotrophicum* and *Desulfocapsa* sp., as identified by 16S rRNA gene sequencing, are known to grow as chemolithoautotrophs by performing $H_2$ oxidation or $S^0$ disproportionation (43, 44) (Fig. 6) and are important contributors to the chemolithoautotrophic activity in coastal sediments (11, 45). However, a further identification of the chemolithoautotrophic *Deltaproteobacteria* through the functional genes related to carbon fixation pathways was not performed in this study. Although it is known that autotrophic *Deltaproteobacteria* mainly use the reverse TCA cycle or the reductive acetyl-coenzyme A (acetyl-CoA) pathway (27), further development of the functional gene approach by designing specific primers is necessary to determine and clarify the diversity of *Deltaproteobacteria* involved in the chemolithoautotrophic activity.

Overall, we hypothesize that such a diverse assemblage of chemolithoautotrophic bacteria in the presence of cable bacteria is indicative of a complex niche partitioning among these sulfur oxidizers (*Gammaproteobacteria*, *Epsilonproteobacteria*, and *Deltaproteobacteria*). In sulfidic marine sediments found in tidal and deep-sea habitats, complex $S^0$ niche partitioning has been proposed where uncultured sulfur-oxidizing *Gammaproteobacteria* mainly thrive on free sulfide, the epsilonproteobacterial *Sulfurimonas*/*Sulfurovum* group oxidizes elemental sulfur, and members of the deltaproteobacterial *Desulfobulbaceae* family may perform $S^0$ disproportionation (46).

**Nitrate-storing filamentous *Beggiatoaceae*.** Nitrate-storing filamentous *Beggiatoaceae* glide through the sediment, transporting their electron acceptor (intracellular vacuoles filled with high concentrations of $NO_3^-$) into deeper sediment and electron donor (intracellular granules of elemental sulfur) up to the surface; in doing so, they oxidize free sulfide to sulfate in a two-step process that creates a wide suboxic zone (14, 47, 48) (Fig. 6). In March, the microsensor depth profiles at S2 (Fig. 1a) revealed a centimeter-thick suboxic zone with a subsurface pH minimum at the OPD, followed by a pH maximum at SAD, which is the characteristic geochemical fingerprint of sulfur oxidation by nitrate-storing *Beggiatoaceae* (14, 48). At the same time, microscopy revealed high biovolumes of *Beggiatoaceae* that were uniformly distributed throughout

Downloaded from http://aem.asm.org/ on July 12, 2018 by Universiteitsbibliotheek Utrecht

the suboxic zone (Fig. 1c), and more than half the filaments found were thicker than 15 $\mu$m, indicating potential nitrate storage. Together, these results corroborate the indications of the dominant sulfur oxidation mechanism suggested by the geochemical fingerprint.

The chemolithoautotrophy depth profile at S2 in March (Fig. 1b) recorded higher activities in the top 1 cm, and chemolithoautotrophic activity penetrated down only to 2 cm (at the sulfide appearance depth). The similar depth distributions of *Beggiatoaceae* and chemolithoautotrophic activity suggest that dark $CO_2$ fixation was primarily carried out by the nitrate-storing *Beggiatoaceae*. *Beggiatoaceae* can indeed grow as obligate or facultative chemolithoautotrophs, depending on the strain (49). The PLFA-SIP analysis further supported chemolithoautotrophy by *Beggiatoaceae*, as the PLFA patterns obtained at S2 resembled those of *Beggiatoa* mats encountered in sediments associated with gas hydrates (41).

However, the $CO_2$ fixation by *Beggiatoaceae* could be complemented by the activity of other chemolithoautotrophs. *Beggiatoaceae* have previously been reported to cooccur with chemolithoautotrophic nitrate-reducing and sulfur-oxidizing *Epsilonproteobacteria* (*Sulfurovum* and *Sulfurimonas*) in the deep-sea Guyamas basin (50). Interestingly, station S2 in March showed the highest number of *aclB* gene copies of all stations and seasons (Fig. 4b), and it had the highest relative percentage of 16S rRNA gene read sequences assigned to the *Epsilonproteobacteria* (Fig. 2). Therefore, the dark $CO_2$ fixation at station S2 is likely caused by both the motile vacuolated *Beggiatoaceae* as well as the sulfur-oxidizing *Epsilonproteobacteria*. Yet, as was the case with the cable bacteria mentioned above, the metabolic link between *Beggiatoaceae* and the *Epsilonproteobacteria* remains unknown. However, it seems possible that internally stored $NO_3^-$ is released into the sediment once *Beggiatoa* filaments lyse, allowing sulfur oxidation with $NO_3^-$ by *Epsilonproteobacteria*.

**Summer activity and diversity of chemolithoautotrophic bacteria.** In August, when the $O_2$ levels in the bottom water decreased substantially, a third geochemical regime was observed at all stations, which was different from the regimes associated with cable bacteria or nitrate-storing *Beggiatoaceae*. The microsensor profiling revealed an upward diffusive transport of free sulfide to the top millimeters of the sediment, which was produced in deeper sediment horizons through sulfate reduction (Fig. 1a). The uniform decrease in pH with depth is consistent with sediments dominated by sulfate reduction (39). As noted above, the chemolithoautotrophy rates strongly decreased compared to March and were restricted to the very top of the sediment. Chemolithoautotrophic activity showed a close relationship with the bottom-water oxygen concentration. The number of gene copies of the two carbon fixation pathways investigated (CBB and rTCA) also decreased under hypoxic conditions (Fig. 4), suggesting a strong dependence of subsurface chemolithoautotrophy on the availability of oxygen in bottom waters.

The highest chemolithoautotrophy rate was recorded at the shallower station (S3), which was the only station in August where $O_2$ was found to diffuse into the sediment (Table 1), thus supporting aerobic sulfur oxidation at a shallow oxic-sulfidic interface in the sediment (39). Several studies have shown that chemolithoautotrophy ceases in the absence of oxygen in the overlying water column (15, 32, 45). Such full anoxia occurred in the deepest station (S1), but limited chemolithoautotrophic activity was still recorded in the top layer of the sediment. A possible explanation is that some residual aerobic sulfur-oxidizing bacteria were supported by the very low oxygen levels. Alternatively, cable bacteria activity at S1 in spring leads to a buildup of iron (hydr)oxides (FeOOH) in the top of the sediments, which prevents sulfide diffusion to the bottom-water during summer anoxia ($3H_2S + 2FeOOH \rightarrow 2FeS + S^0 + 4H_2O$) (14). The elemental sulfur formed in this reaction may support chemolithoautotrophic sulfur-disproportionating bacteria (43). At station S2, *Beggiatoaceae* were found forming a mat at the sediment surface at S2 (Fig. 1b), and chemolithoautotrophic activity was limited to this mat (Fig. 6). *Beggiatoaceae* can survive hypoxic periods by using

Downloaded from http://aem.asm.org/ on July 12, 2018 by Universiteitsbibliotheek Utrecht

stored nitrate as an electron acceptor (51), which is thought to be a competitive advantage that leads to their proliferation in autumn at S1 (14). Such survival strategies may be used to produce energy for maintenance rather than growth under hypoxic conditions, which would, in combination with the low oxygen concentrations, explain the low chemolithoautotrophy-to-biovolume ratio observed at S2 in August compared to that in March.

**Conclusion.** Coastal sediments harbor a great potential for chemolithoautotrophic activity given the high anaerobic mineralization and produce a large pool of reduced sulfur in these organic-rich sediments. In this study, two environmental factors were identified to regulate the chemolithoautotrophic activity in coastal sediments: seasonal hypoxia and the dominant sulfur oxidation mechanism. In sediments where oxygen, the main electron acceptor for chemolithoautotrophs, is depleted because of seasonal hypoxia, chemolithoautotrophy was strongly inhibited. In addition, it is clear that the different sulfur oxidation mechanism (e.g., canonical sulfur oxidation, electrogenic sulfur oxidation, or sulfur oxidation mediated by vacuolated *Beggiatoaceae*) observed in the sediment also determines the magnitude and depth distribution of the dark $CO_2$ fixation, as well as the chemolithoautotrophic bacterial community structure. The seasonal variations in electron acceptors and potentially reduced sulfur species suggest complex niche partitioning in the sediment by the sulfur-oxidizing bacterial community. An in-depth study on the availability of different sulfur species in the sediment could shed light on the sulfur preferences by the different bacterial groups. Likewise, the potential mechanism used to metabolically link filamentous sulfur oxidizers and chemolithoautotrophic bacteria remains unresolved and requires further study. These tight metabolic relationships may ultimately regulate the cycling of sulfur, carbon, and even nitrogen in coastal sediments, including (but not limited to) sediments affected by seasonal hypoxia.

## MATERIALS AND METHODS

**Study site and sediment sampling.** Lake Grevelingen is a former estuary located within the Rhine-Meuse-Scheldt delta area of The Netherlands, which became a closed saline reservoir (salinity, ~30) by dam construction at both the land side and sea side in the early 1970s. Due to an absence of tides and strong currents, Lake Grevelingen experiences a seasonal stratification of the water column, which in turn leads to a gradual depletion of the oxygen in the bottom waters (52). Bottom-water oxygen at the deepest stations typically starts to decline in April, reaches hypoxic conditions by end of May ($O_2$ concentration, $<63$ $\mu$M), further decreasing to anoxia in August (O concentration, $<0.1$ $\mu$M), and reoxygenation of the bottom water takes place in September (14).

To study the effects of the bottom-water oxygenation on the benthic chemolithoautotrophic community, we performed a field sampling campaign on 13 March 2012 (before the start of the annual $O_2$ depletion) and 20 August 2012 (at the height of the annual $O_2$ depletion). Details of the water column, pore water, and solid sediment chemistry of Lake Grevelingen over the year 2012 have been previously reported (14, 26, 52). Sediments were recovered at three stations along a depth gradient within the Den Osse basin, one of the deeper basins in Lake Grevelingen: station 1 (S1) was located at the deepest point (34 m) of the basin (51.747°N, 3.890°E), station 2 (S2) was located at 23 m depth (51.749°N, 3.897°E), and station 3 (S3) was located at 17 m depth (51.747°N, 3.898°E). Intact sediment cores were retrieved with a single-core gravity corer (Uwitec) using polyvinyl chloride (PVC) core liners (6-cm inner diameter and 60-cm length). All cores were inspected upon retrieval, and only cores with a visually undisturbed surface were used for further analysis.

Thirteen sediment cores for microbial analysis were collected per station and per time point: two cores for phospholipid-derived fatty acid analysis combined with stable isotope probing (PLFA-SIP), two cores for nucleic acid analysis, four cores for [$^{13}$C]bicarbonate labeling, three cores for microelectrode profiling, one core for quantification of cable bacteria (see supplemental material), and one core for quantification of *Beggiatoaceae* (see supplemental material). Sediment cores for PLFA extractions were sliced manually on board the ship (5 sediment layers; sectioning at 0.5, 1, 2, 4, and 6 cm depth). Sediment slices were collected in petri dishes, and replicate depths were pooled and thoroughly mixed. Homogenized sediments were immediately transferred to centrifuge tubes (50 ml) and placed in dry ice until further analysis. Surface sediments in August consisted of a highly porous "fluffy" layer that was first left to settle after core retrieval. Afterwards, the top 1-cm-thick layer was recovered through suction (rather than slicing). Sediment for nucleic acid analysis was collected by slicing manually at a resolution of 1 cm up to 5 cm depth. Sediment samples were frozen in dry ice, transported to the laboratory within a few hours, and placed at −80°C until further analysis.

**Microsensor profiling.** Oxygen depth profiles were recorded with commercial microelectrodes (Unisense, Denmark; tip size, 50 $\mu$m) at 25- to 500$\mu$m resolution. For $H_2S$ and pH (tip size, 50 and 200 $\mu$m), depth profiles were recorded at 200-$\mu$m resolution in the oxic zone and at 400- or 600-$\mu$m-depth

Downloaded from http://aem.asm.org/ on July 12, 2018 by Universiteitsbibliotheek Utrecht

resolution below. Calibrations for $O_2$, pH, and $H_2S$ were performed as previously described (14, 53). $\Sigma H_2S$ was calculated from $H_2S$ based on pH measured at the same depth using the R package AquaEnv (54). The oxygen penetration depth (OPD) is operationally defined as the depth below which the [$O_2$] is $<1$ $\mu$M, while the sulfide appearance depth (SAD) is operationally defined as the depth below which the [$H_2S$] is $>1$ $\mu$M. The diffusive oxygen uptake (DOU) was calculated from the oxygen depth profiles, as previously described in detail (15).

**DNA extraction and 16S rRNA gene amplicon sequencing.** DNA from 0-cm to 5-cm sediment depth (at 1-cm resolution) was extracted using the DNA PowerSoil total isolation kit (Mo Bio Laboratories, Inc., Carlsbad, CA). Nucleic acid concentrations were quantified spectrophotometrically (NanoDrop; Thermo Scientific, Wilmington, DE) and checked by agarose gel electrophoresis for integrity. DNA extracts were kept frozen at −80°C.

Sequencing of 16S rRNA gene amplicons was performed on the first centimeter of the sediment (0 to 1 cm depth) in all stations in March and August, as described before (55). Further details are provided in the supplemental material. The phylogenetic affiliation of the 16S rRNA gene sequences was compared to release 119 of the Silva SSU Ref NR database (http://www.arb-silva.de/) (56) using the ARB software package (57). Sequences were added to a reference tree generated from the Silva database using the ARB parsimony tool.

**Sediment incubations and PLFA-SIP analysis.** Sediment cores were labeled with [$^{13}$C]bicarbonate to determine the chemolithoautotrophic activity and associated bacterial community by tracing the incorporation of $^{13}$C into bacterial PLFA. To this end, four intact cores were subcored with smaller core liners (4.5-cm inner diameter and 20-cm height). *In situ* bottom water was kept over the sediment, and no gas headspace was present. Cores were kept inside a closed cooling box during transport to the laboratory.

Stock solutions of 80 mM [$^{13}$C]bicarbonate (99% $^{13}$C; Cambridge Isotope Laboratories, Andover, MA, USA) were prepared as previously described (11). [$^{13}$C]Bicarbonate was added to the sediment from 3 cm above the surface to 8 cm deep in the sediment cores in aliquots of 100 $\mu$l through vertically aligned side ports (0.5 cm apart) with the line injection method (58). March sediments were incubated at 17 $\pm$ 1°C in the dark for 24 h and continuously aerated with $^{13}$C-saturated air to maintain 100% saturated $O_2$ conditions, like those found *in situ*, but avoiding the stripping of labeled $CO_2$ from the overlying water (15). In August, sediments were incubated at 17 $\pm$ 1°C in the dark for 40 h to ensure sufficient labeling, as a lower activity was expected under low oxygen concentrations. In August, oxygen concentrations in the overlying water were maintained near *in situ* $O_2$ levels measured in the bottom water (S1, 0 to 4% saturation; S2, 20 to 26% saturation; S3, 35 to 80% saturation). A detailed description of the aeration procedures can be found in the supplemental material.

At the end of the incubation period, sediment cores were sliced in five depth intervals (as described for PLFA sediment cores sliced on board), thus obtaining two replicate slices per sediment depth and per station. Sediment layers were collected in centrifuge tubes (50 ml), and wet volume and weight were noted. Pore water was obtained by centrifugation (4,500 rpm for 5 min) for dissolved inorganic carbon (DIC) analysis, and sediments were lyophilized for PLFA analysis. Biomarker extractions were performed on freeze-dried sediment, as described before (59) and $^{13}$C incorporation into PLFA was analyzed as previously reported (11). Nomenclature of PLFA can be found in the supplemental material. A detailed description of the PLFA calculations can be found in the literature (15, 35). Total dark $CO_2$ fixation rates (in nanomoles carbon per meter squared per day) are the depth-integrated rates obtained from the 0- to 6-cm sediment interval.

**Quantitative PCR.** To determine the abundance of chemolithoautotrophs, we quantified the genes coding for two enzymes involved in dark $CO_2$ fixation pathways: the large subunit of the RuBisCO enzyme (ribulose 1,5-bisphosphate carboxylase/oxygenase) *cbbL* gene, and the ATP citrate lyase *aclB* gene. The abundance of the RuBisCO *cbbL* gene was estimated by using primers K2f/V2r, specific for forms IA and IC of the RuBisCO form I large subunit gene *cbbL*, which is present in obligately and facultatively lithotrophic bacteria (24, 60). The abundance of the ATP citrate lyase *aclB* gene was quantified by using the primer set aclB_F/aclB_R, which is based on the primers 892F/1204R (61) specific for the ATP citrate lyase $\beta$ gene of chemoautotrophic bacteria using the rTCA pathway, with several nucleotide differences introduced after aligning $n = 100$ sequences of *aclB* gene fragments affiliated with *Epsilonproteobacteria* (see Table S1 for details).

The quantification of *cbbL* and *aclB* genes via quantitative PCR (qPCR) was performed at 1-cm resolution for the sediment interval between 0 and 5 cm depth in all stations in both March and August. qPCR analyses were performed on a Bio-Rad CFX96 real-time system/C1000 thermal cycler equipped with the CFX Manager software. All qPCRs were performed in triplicate with standard curves from $10^0$ to $10^7$ molecules/$\mu$l. Standard curves and qPCRs were performed as previously described (62). Melting temperatures ($T_m$) are listed in Table S1, and qPCR efficiencies ($E$) for *aclB* gene and *cbbL* gene amplifications were 70 and 82%, respectively. Correlation coefficients for standard curves were $\geq$0.994 for *aclB* gene amplification and $\geq$0.988 for *cbbL* gene amplification.

**PCR amplification and cloning.** Amplifications of the RuBisCO *cbbL* gene and the ATP citrate lyase *aclB* gene were performed with the primer pairs specified in Table S1. The PCR mixture was the following (final concentration): 1× Q-solution (PCR additive; Qiagen, Valencia, CA), 1× PCR buffer, bovine serum albumin (BSA; 200 $\mu g \cdot ml^{-1}$), dinucleoside triphosphates (dNTPs; 20 $\mu$M), primers (0.2 pmol $\cdot$ $\mu l^{-1}$), $MgCl_2$ (1.5 mM), and 1.25 U of *Taq* polymerase (Qiagen). The PCR conditions for these amplifications were the following: 95°C for 5 min; 35 cycles of 95°C for 1 min, $T_m$ for 1 min, and 72°C for 1 min; and a final extension of 72°C for 5 min. PCR products were gel purified (QIAquick gel purification kit; Qiagen), cloned in the TOPO-TA cloning kit (Life Technologies, Carlsbad, CA), and transformed in *Escherichia coli* TOP10

Downloaded from http://aem.asm.org/ on July 12, 2018 by Universiteitsbibliotheek Utrecht

cells, according to the manufacturer's recommendations. Recombinant plasmid DNA was sequenced using the M13R primer by BaseClear (Leiden, The Netherlands).

Sequences were aligned with the MEGA5 software (63) by using the alignment method ClustalW. The phylogenetic trees of the *cbbL* and *aclB* genes were computed with the neighbor-joining method (64). The evolutionary distances were estimated using the Jukes-Cantor method (65) for DNA sequences, and with the Poisson correction method for protein sequences (66), with a bootstrap test of 1,000 replicates.

Further details on the experimental procedures and methods are found in the supplemental material.

**Accession number(s).** Sequences were deposited in NCBI with the accession numbers KT328918 to KT328956 for *cbbL* gene sequences and KT328957 to KT329097 for *aclB* gene sequences. The 16S rRNA gene amplicon reads (raw data) have been deposited in the NCBI Sequence Read Archive (SRA) under BioProject no. PRJNA293286.

## SUPPLEMENTAL MATERIAL

Supplemental material for this article may be found at https://doi.org/10.1128/AEM.03517-16.

**SUPPLEMENTAL FILE 1,** PDF file, 1.0 MB.

## ACKNOWLEDGMENTS

We thankfully acknowledge the crew of the R/V *Luctor* (Peter Coomans and Marcel Kristalijn) and Pieter van Rijswijk for their help in the field during sediment collection, Marcel van der Meer and Sandra Heinzelmann for support onboard and assistance with incubations, Peter van Breugel and Marco Houtekamer for their assistance with stable isotope analysis, Elda Panoto for technical support, and Alexandra Vasquez Cardenas for designing Fig. 6.

This work was financially supported by several grants from the Darwin Centre for Biogeosciences to H.T.S.B. (grant 3061), L.V. (grant 3062), and F.J.R.M. (grant 3092). F.J.R.M. received funding from the European Research Council under the European Union's Seventh Framework Program (FP7/2007-2013) via ERC grant 306933, and R.S. received support from the Danish Council for Independent Research-Natural Sciences.

## REFERENCES

1. Soetaert K, Herman PMJ, Middelburg JJ. 1996. A model of early diagenetic processes from the shelf to abyssal depths. Geochim Cosmochim Acta 60:1019–1040. https://doi.org/10.1016/0016-7037(96)00013-0.
2. Jørgensen BB, Nelson DC. 2004. Sulfide oxidation in marine sediments: geochemistry meets microbiology. Geol Soc Am 379:61–81.
3. Howarth WR. 1984. The ecological significance of sulfur in the energy dynamics of salt marsh and coastal marine sediments. Biogeochemistry 1:5–27. https://doi.org/10.1007/BF02181118.
4. Brüchert V, Jørgensen BB, Neumann K, Riechmann D, Schlösser M, Schulz H. 2003. Regulation of bacterial sulfate reduction and hydrogen sulfide fluxes in the central Namibian coastal upwelling zone. Geochim Cosmochim Acta 67:4505–4518. https://doi.org/10.1016/S0016-7037(03)00275-8.
5. Lavik G, Stührmann T, Brüchert V, Van der Plas A, Mohrholz V, Lam P, Mußmann M, Fuchs BM, Amann R, Lass U, Kuypers MM. 2009. Detoxification of sulphidic African shelf waters by blooming chemolithotrophs. Nature 457:581–584. https://doi.org/10.1038/nature07588.
6. Sorokin DY, Kuenen JG, Muyzer G. 2011. The microbial sulfur cycle at extremely haloalkaline conditions of soda lakes. Front Microbiol 2:44. https://doi.org/10.3389/fmicb.2011.00044.
7. Grote J, Schott T, Bruckner CG, Glöckner FO, Jost G, Teeling H, Labrenz M, Jürgens K. 2012. Genome and physiology of a model epsilonproteobacterium responsible for sulfide detoxification in marine oxygen depletion zones. Proc Natl Acad Sci U S A 109:506–510. https://doi.org/10.1073/pnas.1111262109.
8. Jessen GL, Lichtschlag A, Struck U, Boetius A. 2016. Distribution and composition of thiotrophic mats in the hypoxic zone of the Black Sea (150–170 m water depth, Crimea Margin). Front Microbiol 7:1011. https://doi.org/10.3389/fmicb.2016.01011.
9. Ye Q, Wu Y, Zhu Z, Wang X, Li Z, Zhang J. 2016. Bacterial diversity in the surface sediments of the hypoxic zone near the Changjiang Estuary and in the East China Sea. Microbiologyopen 5:323–339. https://doi.org/10.1002/mbo3.330.
10. Lenk S, Arnds J, Zerjatke K, Musat N, Amann R, Mußmann M. 2010. Novel groups of Gammaproteobacteria catalyse sulfur oxidation and carbon fixation in a coastal, intertidal sediment. Environ Microbiol 13:758–774. https://doi.org/10.1111/j.1462-2920.2010.02380.x.
11. Boschker HT, Vasquez-Cardenas D, Bolhuis H, Moerdijk-Poortvliet TW, Moodley L. 2014. Chemoautotrophic carbon fixation rates and active bacterial communities in intertidal marine sediments. PLoS One 9:e101443. https://doi.org/10.1371/journal.pone.0101443.
12. Dyksma S, Bischof K, Fuchs BM, Hoffmann K, Meier D, Meyerdierks A, Pjevac P, Probandt D, Richter M, Stepanauskas R, Mußmann M. 2016. Ubiquitous Gammaproteobacteria dominate dark carbon fixation in coastal sediments. ISME J 10:1939–1953. https://doi.org/10.1038/ismej.2015.257.
13. Diaz RJ, Rosenberg R. 2008. Spreading dead zones and consequences for marine ecosystems. Science 321:926–929. https://doi.org/10.1126/science.1156401.
14. Seitaj D, Schauer R, Sulu-Gambari F, Hidalgo-Martinez S, Malkin SY, Burdorf LDW, Slomp CP, Meysman FJR. 2015. Cable bacteria generate a firewall against euxinia in seasonally hypoxic basins. Proc Natl Acad Sci U S A 43:13278–13283. https://doi.org/10.1073/pnas.1510152112.
15. Vasquez-Cardenas D, van de Vossenberg J, Polerecky L, Malkin SY, Schauer R, Hidalgo-Martinez S, Confurius V, Middelburg JJ, Meysman FJ, Boschker HTS. 2015. Microbial carbon metabolism associated with electrogenic sulphur oxidation in coastal sediments. ISME J 9:1966–1978. https://doi.org/10.1038/ismej.2015.10.
16. Nelson DC, Jannasch HW. 1983. Chemoautotrophic growth of a marine *Beggiatoa* in sulfide-gradient cultures. Arch Microbiol 136:262–269. https://doi.org/10.1007/BF00425214.
17. Bowman JP, McMeekin TA. 2005. Order X, Alteromonadales ord. nov., p 443–491. *In* Brenner D, Krieg N, Staley J, Garrity G (ed), Bergey's manual of systematic bacteriology, 2nd ed. vol 2. Springer, New York, NY.
18. Salman V, Amann R, Girnth AC, Polerecky L, Bailey JV, Høgslund S, Jessen G, Pantoja S, Schulz-Vogt HN. 2011. A single-cell sequencing approach to the classification of large, vacuolated sulfur bacteria. Syst Appl Microbiol 34:243–259. https://doi.org/10.1016/j.syapm.2011.02.001.

Downloaded from http://aem.asm.org/ on July 12, 2018 by Universiteitsbibliotheek Utrecht

19. Salman V, Bailey JV, Teske A. 2013. Phylogenetic and morphologic complexity of giant sulphur bacteria. Antonie Van Leeuwenhoek 104:169–186. https://doi.org/10.1007/s10482-013-9952-y.
20. Campbell BJ, Engel AS, Porter ML, Takai K. 2006. The versatile ε-proteobacteria: key players in sulphidic habitats. Nat Rev Microbiol 4:458–468. https://doi.org/10.1038/nrmicro1414.
21. Inagaki F, Takai K, Kobayashi H, Nealson K, Horikoshi K. 2003. *Sulfurimonas autotrophica* gen. nov., sp. nov., a novel sulfur-oxidizing epsilonproteobacterium isolated from hydrothermal sediments in the Mid-Okinawa Trough. Int J Syst Evol Microbiol 53:1801–1805. https://doi.org/10.1099/ijs.0.02682-0.
22. Donachie SP, Bowman JP, On SLW, Alam M. 2005. *Arcobacter halophilus* sp. nov., the first obligate halophile in the genus *Arcobacter*. Int J Syst Evol Microbiol 55:1271–1277. https://doi.org/10.1099/ijs.0.63581-0.
23. Berg IA. 2011. Ecological aspects of the distribution of different autotrophic $CO_2$ fixation pathways. Appl Environ Microbiol 77:1925–1936. https://doi.org/10.1128/AEM.02473-10.
24. Nigro LM, King GM. 2007. Disparate distributions of chemolithotrophs containing form IA or IC large subunit genes for ribulose-1,5-bisphosphate carboxylase/oxygenase in intertidal marine and littoral lake sediments. FEMS Microbiol Ecol 60:113–125. https://doi.org/10.1111/j.1574-6941.2007.00272.x.
25. Schauer R, Risgaard-Petersen N, Kjeldsen KU, Tataru Bjerg JJ, Jørgensen BB, Schramm A, Nielsen LP. 2014. Succession of cable bacteria and electric currents in marine sediment. ISME J 8:1314–1322. https://doi.org/10.1038/ismej.2013.239.
26. Sulu-Gambari F, Seitaj D, Meysman FJR, Schauer R, Polerecky L, Slomp CP. 2016. Cable bacteria control iron-phosphorus dynamics in sediments of a coastal hypoxic basin. Environ Sci Technol 50:1227–1233. https://doi.org/10.1021/acs.est.5b04369.
27. Hügler M, Sievert SM. 2011. Beyond the Calvin cycle: autotrophic carbon fixation in the ocean. Annu Rev Mar Sci 3:261–289. https://doi.org/10.1146/annurev-marine-120709-142712.
28. Sorokin DY, Lysenko AM, Mityushina LL, Tourova TP, Jones BE, Rainey FA, Robertson LA, Kuenen GJ. 2001. *Thioalkalimicrobium aerophilum* gen. nov., sp. nov. and *Thioalkalimicrobium sibericum* sp. nov., and *Thioalkalivibrio versutus* gen. nov., sp. nov., *Thioalkalivibrio nitratis* sp. nov. and *Thioalkalivibrio denitrificans* sp. nov., novel obligately alkaliphilic and obligately chemolithoautotrophic sulfur-oxidizing bacteria from soda lakes. Int J Syst Evol Microbiol 51:565–580. https://doi.org/10.1099/00207713-51-2-565.
29. Takai K, Suzuki M, Nakagawa S, Miyazaki M, Suzuki Y, Inagaki F, Horikoshi K. 2006. *Sulfurimonas paralvinellae* sp. nov., a novel mesophilic, hydrogen- and sulfur-oxidizing chemolithoautotroph within the *Epsilonproteobacteria* isolated from a deep-sea hydrothermal vent polychaete nest, reclassification of *Thiomicrospira denitrificans* as *Sulfurimonas denitrificans* comb. nov. and emended description of the genus *Sulfurimonas*. Int J Syst Evol Microbiol 56:1725–1733. https://doi.org/10.1099/ijs.0.64255-0.
30. Labrenz M, Grote J, Mammitzsch K, Boschker HTS, Laue M, Jost G, Glaubitz S, Jürgens K. 2013. *Sulfurimonas gotlandica* sp. nov., a chemoautotrophic and psychrotolerant epsilonproteobacterium isolated from a pelagic redoxcline, and an emended description of the genus *Sulfurimonas*. Int J Syst Evol Microbiol 63:4141–4148. https://doi.org/10.1099/ijs.0.048827-0.
31. Llobet-Brossa E, Rabus R, Böttcher ME, Könneke M, Finke N, Schramm A, Meyer RL, Grötzschel S, Rosselló-Mora R, Amann R. 2002. Community structure and activity of sulfate-reducing bacteria in an intertidal surface sediment: a multi-method approach. Aquat Microb Ecol 29:211–226. https://doi.org/10.3354/ame029211.
32. Miyatake T. 2011. Linking microbial community structure to biogeochemical function in coastal marine sediments. Ph.D. dissertation. University of Amsterdam, Amsterdam, The Netherlands.
33. Muyzer G, Stams AJM. 2008. The ecology and biotechnology of sulphate-reducing bacteria. Nat Rev Microbiol 6:441–456.
34. Vestal JR, White DC. 1989. Lipid analysis in microbial ecology: quantitative approaches to the study of microbial communities. Bioscience 39:535–541. https://doi.org/10.2307/1310976.
35. Boschker HTS, Middelburg JJ. 2002. Stable isotopes and biomarkers in microbial ecology. FEMS Microbiol Ecol 40:85–95. https://doi.org/10.1111/j.1574-6941.2002.tb00940.x.
36. Taylor J, Parkes RJ. 1983. The cellular fatty acids of the sulphate-reducing bacteria, *Desulfobacter* sp., *Desulfobulbus* sp. and *Desulfovibrio desulfuricans*. J Gen Microbiol 129:3303–3309.
37. Edlund A, Nichols PD, Roffey R, White DC. 1985. Extractable and lipopolysaccharide fatty acid and hydroxy acid profiles from *Desulfovibrio* species. J Lipid Res 26:982–988.
38. Nielsen LP, Risgaard-Petersen N, Fossing H, Christensen PB, Sayama M. 2010. Electric currents couple spatially separated biogeochemical processes in marine sediment. Nature 463:1071–1074. https://doi.org/10.1038/nature08790.
39. Meysman FJR, Risgaard-Petersen N, Malkin SY, Nielsen LP. 2015. The geochemical fingerprint of microbial long-distance electron transport in the seafloor. Geochim Cosmochim Acta 152:122–142. https://doi.org/10.1016/j.gca.2014.12.014.
40. Pfeffer C, Larsen S, Song J, Dong M, Besenbacher F, Meyer RL, Kjeldsen KU, Schreiber L, Gorby YA, El-Naggar MY, Leung KM, Schramm A, Risgaard-Petersen N, Nielsen LP. 2012. Filamentous bacteria transport electrons over centimetre distances. Nature 491:218–221. https://doi.org/10.1038/nature11586.
41. Zhang CL, Huang Z, Cantu J, Pancost RD, Brigmon RL, Lyons TW, Sassen R. 2005. Lipid biomarkers and carbon isotope signatures of a microbial (*Beggiatoa*) mat associated with gas hydrates in the Gulf of Mexico. Appl Environ Microbiol 71:2106–2112. https://doi.org/10.1128/AEM.71.4.2106-2112.2005.
42. Webster G, Watt LC, Rinna J, Fry JC, Evershed RP, Parkes RJ, Weightman AJ. 2006. A comparison of stable-isotope probing of DNA and phospholipid fatty acids to study prokaryotic functional diversity in sulfate-reducing marine sediment enrichment slurries. Environ Microbiol 8:1575–1589. https://doi.org/10.1111/j.1462-2920.2006.01048.x.
43. Finster K, Liesack W, Thamdrup B. 1998. Elemental sulfur and thiosulfate disproportionation by *Desulfocapsa sulfoexigens* sp. nov., a new anaerobic bacterium isolated from marine surface sediment. Appl Environ Microbiol 64:119–125.
44. Böttcher ME, Thamdrup B, Gehre M, Theune A. 2005. $^{34}S/^{32}S$ and $^{18}O/^{16}O$ fractionation during sulfur disproportionation by *Desulfobulbus propionicus*. Geomicrobiol J 22:219–226. https://doi.org/10.1080/01490450590947751.
45. Thomsen U, Kristensen E. 1997. Dynamics of $\Sigma CO_2$ in a surficial sandy marine sediment: the role of chemoautotrophy. Aquat Microb Ecol 12:165–176. https://doi.org/10.3354/ame012165.
46. Pjevac P, Kamyshny A, Dyksma S, Mußmann M. 2014. Microbial consumption of zero-valence sulfur in marine benthic habitats. Environ Microbiol 16:3416–3430. https://doi.org/10.1111/1462-2920.12410.
47. Mussmann M, Schulz HN, Strotmann B, Kjær T, Nielsen LP, Rosselló-Mora RA, Amann RI, Jørgensen BB. 2003. Phylogeny and distribution of nitrate-storing *Beggiatoa* spp. in coastal marine sediments. Environ Microbiol 5:523–533. https://doi.org/10.1046/j.1462-2920.2003.00440.x.
48. Sayama M, Risgaard-Petersen N, Nielsen LP, Fossing H, Christensen PB. 2005. Impact of bacterial $NO3^-$ transport on sediment biogeochemistry. Appl Environ Microbiol 71:7575–7577. https://doi.org/10.1128/AEM.71.11.7575-7577.2005.
49. Hagen KD, Nelson DC. 1996. Organic carbon utilization by obligately and facultatively autotrophic beggiatoa strains in homogeneous and gradient cultures. Appl Environ Microbiol 62:947–953.
50. Bowles MW, Nigro LM, Teske AP, Joye SB. 2012. Denitrification and environmental factors influencing nitrate removal in Guaymas Basin hydrothermally altered sediments. Front Microbiol 3:377. https://doi.org/10.3389/fmicb.2012.00377.
51. Schulz HN, Jørgensen BB. 2001. Big bacteria. Annu Rev Microbiol 55:105–137. https://doi.org/10.1146/annurev.micro.55.1.105.
52. Hagens M, Slomp CP, Meysman FJR, Seitaj D, Harlay J, Borges AV, Middelburg JJ. 2015. Biogeochemical processes and buffering capacity concurrently affect acidification in a seasonally hypoxic coastal marine basin. Biogeosciences 12:1561–1583. https://doi.org/10.5194/bg-12-1561-2015.
53. Malkin SY, Rao AM, Seitaj D, Vasquez-Cardenas D, Zetsche E-M, Hidalgo-Martinez S, Boschker HTS, Meysman FJR. 2014. Natural occurrence of microbial sulphur oxidation by long-range electron transport in the seafloor. ISME J 8:1843–1854. https://doi.org/10.1038/ismej.2014.41.
54. Hofmann AF, Soetaert K, Middelburg JJ, Meysman FJR. 2010. AquaEnv: an aquatic acid-base modelling environment in R. Aquat Geochem 16:507–546. https://doi.org/10.1007/s10498-009-9084-1.
55. Moore EK, Villanueva L, Hopmans EC, Rijpstra WIC, Mets A, Dedysh SN, Sinninghe Damsté JS. 2015. Abundant trimethylornithine lipids and specific gene sequences are indicative of planctomycete importance at the oxic/anoxic interface in *Sphagnum*-dominated northern wetlands.


Downloaded from http://aem.asm.org/ on July 12, 2018 by Universiteitsbibliotheek Utrecht

Appl Environ Microbiol 81:6333–6344. https://doi.org/10.1128/AEM.00324-15.
56. Quast C, Pruesse E, Yilmaz P, Gerken J, Schweer T, Yarza P, Peplies J, Glöckner FO. 2013. The SILVA ribosomal RNA gene database project: improved data processing and Web-based tools. Nucleic Acids Res 41:D590-6. https://doi.org/10.1093/nar/gks1219.
57. Ludwig W, Strunk O, Westram R, Richter L, Meier H, Yadhukumar, Buchner A, Lai T, Steppi S, Jobb G, Förster W, Brettske I, Gerber S, Ginhart AW, Gross O, Grumann S, Hermann S, Jost R, König A, Liss T, Lüßmann R, May M, Nonhoff B, Reichel B, Strehlow R, Stamatakis A, Stuckmann N, Vilbig A, Lenke M, Ludwig T, Bode A, Schleifer K-H. 2004. ARB: a software environment for sequence data. Nucleic Acids Res 32:1363–1371. https://doi.org/10.1093/nar/gkh293.
58. Jørgensen BB. 1978. Comparison of methods for the quantification of bacterial sulfate reduction in coastal marine-sediments: measurement with radiotracer techniques. Geomicrobiol J 1:11–27. https://doi.org/10.1080/01490457809377721.
59. Guckert JB, Antworth CP, Nichols PD, White DC. 1985. Phospholipid, ester-linked fatty-acid profiles as reproducible assays for changes in prokaryotic community structure of estuarine sediments. FEMS Microbiol Ecol 31:147–158. https://doi.org/10.1111/j.1574-6968.1985.tb01143.x.
60. Nanba K, King GM, Dunfield K. 2004. Analysis of facultative lithotroph distribution and diversity on volcanic deposits by use of the large subunit of ribulose 1, 5-bisphosphate carboxylase/oxygenase. Appl Environ Microbiol 70:2245–2253. https://doi.org/10.1128/AEM.70.4.2245-2253.2004.
61. Campbell BJ, Stein JL, Cary SC. 2003. Evidence of chemolithoautotrophy in the bacterial community associated with *Alvinella pompejana*, a hydrothermal vent polychaete. Appl Environ Microbiol 69:5070–5078. https://doi.org/10.1128/AEM.69.9.5070-5078.2003.
62. Lipsewers YA, Bale NJ, Hopmans EC, Schouten S, Sinninghe Damsté JS, Villanueva L. 2014. Seasonality and depth distribution of the abundance and activity of ammonia oxidizing microorganisms in marine coastal sediments (North Sea). Front Microbiol 5:472. https://doi.org/10.3389/fmicb.2014.00472.
63. Tamura K, Peterson D, Peterson N, Stecher G, Nei M, Kumar S. 2011. MEGA5: Molecular Evolutionary Genetics Analysis using maximum likelihood, evolutionary distance, and maximum parsimony methods. Mol Biol Evol 28:2731–2739. https://doi.org/10.1093/molbev/msr121.
64. Saitou N, Nei M. 1987. The neighbor-joining method: a new method for reconstructing phylogenetic trees. Mol Biol Evol 4:406–425.
65. Jukes TH, Cantor CR. 1969. Evolution of proteins, p 21–132. *In* Munro HN (ed), Mammalian protein metabolism. Academic Press, New York, NY.
66. Zuckerkandl E, Pauling L. 1965. Evolutionary divergence and convergence in proteins, p 97–166. *In* Bryson V, Vogel HJ (ed), Evolving genes and proteins. Academic Press, New York, NY.

Downloaded from http://aem.asm.org/ on July 12, 2018 by Universiteitsbibliotheek Utrecht